

and right earlobes, as outlined in Fig. 1. Electrode Cz served as common reference. Vertical and horizontal electro-oculographic (EOG) data were recorded for eye blinks and eye movements. EEG and EOG data were collected for a total period of 4,250 ms, beginning 250 ms before visual-stimulus presentation and continuing for 1,000 ms after the end of a trial. EEG data were corrected for eye movements and eye blinks<sup>23</sup>. Data were sampled online at 200 Hz using a time constant of 10 s.

**Data analysis.** For off-line data analysis, a current-source density (CSD) analysis was performed based on a spherical spline interpolation algorithm using two dimensional Laplace-operators and weighted Legendre polynomials<sup>24–26</sup> in order to maximize the topographic specificity of electrical sources and sinks and to obtain reference-free measures for each electrode<sup>24</sup>. Resulting CSD waveforms were then submitted to a method of coherence analysis involving time-varying autoregressive modelling of multivariate time series based on Kalman filtering<sup>15,27–28</sup>. In the case of single-component signals the use of Kalman filters to fit autoregressive models with time-varying coefficients is common<sup>27–28</sup>. This is possible because such signal models can be given in state-space form. As the Kalman filter can be designed for multi-component signals, we have used a similar state-space form for multi-component autoregressive models with time-varying coefficients. This enables an adaptive estimation of the autoregressive coefficients and derived spectral parameters (that is, coherence) which is suitable for the analysis of non-stationary signals. An order of 16 was chosen for the fitted autoregressive models.

Coherence was computed separately in the bandwidth 37–43 Hz (refs 2, 19), for the delta (0.6–3.5 Hz), theta (3.6–7.5 Hz), alpha 1 (7.6–10 Hz) and alpha 2 (10.1–12.5 Hz) frequency bands, and for additional bands between 30 and 36 Hz, 43 and 48 Hz, and 80 to 100 Hz for the 250-ms time window from 1,250 to 1,500 ms after stimulus onset and the window just before shock onset (that is, 2,750–3,000 ms after stimulus onset). This was also done for the raw EEG. The pairs of electrodes for which analysis was done covered the occipital area (CS<sup>+</sup>, CS<sup>-</sup>), the primary and association somatosensory projection areas (noxious stimulus), and the primary motor areas on both sides of the brain and at the midline. Gamma abundance was also calculated for the frequency band studied in refs 2, 6 (37–43 Hz). Coherence measures were transformed using Fisher's z-transformation and collapsed to obtain mean coherence measures for each subject, each pair of electrodes and each condition of visual stimulation.

**Preference for colours of CS<sup>+</sup> and CS<sup>-</sup>.** Data on colour preference were obtained by questionnaire for the two colours (red and green) assigned randomly to CS<sup>+</sup> and CS<sup>-</sup> before, during, and at the end of acquisition and during and at the end of extinction. The colour-preference data were submitted to a repeated-measures analysis of variance and analysed as a function of condition (CS<sup>+</sup>, CS<sup>-</sup>), and time (beginning, during and end of acquisition, and during and end of extinction). Results were corrected for violation of sphericity using the Greenhouse–Geisser approach to epsilon correction of degrees of freedom. There was a significant effect for condition ( $F(1, 18) = 6.64$ ,  $P < 0.02$ ), time ( $F(4, 72) = 10.43$ ,  $P < 0.0001$ ,  $e = 0.60$ ), and the condition  $\times$  time interaction ( $F(4, 72) = 9.14$ ,  $P < 0.0001$ ,  $e = 0.751$ ), indicating that learning of the association between colour and electric shock had taken place. CS<sup>+</sup> was perceived as most aversive during training, whereas during extinction the difference in preference for CS<sup>+</sup> over CS<sup>-</sup> had almost disappeared.

Received 12 October; accepted 1 December 1998.

1. Hebb, D. O. *The Organization of Behavior* (Wiley, New York, 1949).
2. Singer, W. & Gray, C. M. Visual feature integration and the temporal correlation hypothesis. *Annu. Rev. Neurosci.* **18**, 555–586 (1995).
3. Basar, E., Basar-Eroglu, C. & Schürmann, M. Sensory and cognitive components of brain resonance responses. *Acta Otolaryngol (Stockh.)* **491**, 25–35 (1991).
4. Engel, A. K., König, P., Kreiter, A. K. & Singer, W. Interhemispheric synchronization of oscillatory neuronal responses in cat visual cortex. *Science* **252**, 1177–1179 (1991).
5. Pantev, C. Evoked and induced gamma-band activity of the human cortex. *Brain Topogr.* **7**, 321–330 (1995).
6. Singer, W. The formation of cooperative cell assemblies in the visual cortex. *J. Exp. Biol.* **153**, 177–197 (1990).
7. Pulvermüller, F., Lutzenberger, W., Preißl, H. & Birbaumer, N. Spectral responses in the gamma-band: physiological signs of higher cognitive processes? *Neuroreport* **6**, 2059–2064 (1995).
8. Murthy, V. N., Aoki, F. & Fetz, E. E. In *Oscillatory Event-Related Brain Dynamics* (eds Pantev, C., Elbert, T. & Lütkenhöner, B.) 213–226 (Plenum, New York, 1994).
9. Llinas, R. R. & Ribary, U. Coherent 40-Hz oscillation characterizes dream state in humans. *Proc. Natl. Acad. Sci. USA* **90**, 2078–2081 (1993).
10. Sheer, D. E. In *Self-regulation of the Brain and Behavior* (eds Elbert, T., Rockstroh, B., Lutzenberger, W. & Birbaumer, N.) 64–84 (Springer, Berlin, 1984).
11. Steriade, M., Amzica, F. & Contreras, D. Synchronization of fast (30–40 Hz) spontaneous cortical rhythms during brain activation. *J. Neurosci.* **16**, 392–417 (1996).

12. Tiitinen, H. et al. Selective attention enhances the auditory 40-Hz transient response in humans. *Nature* **364**, 59–60 (1993).
13. Oldfield, R. C. The assessment and analysis of handedness: the Edinburgh inventory. *Neuropsychology* **9**, 97–113 (1971).
14. Pulvermüller, F., Birbaumer, N., Lutzenberger, W. & Mohr, B. High-frequency brain activity: its possible role in attention, perception and language processing. *Prog. Neurobiol.* **52**, 427–445 (1997).
15. Arnold, M., Miltner, W. H. R., Bauer, R. & Braun, C. Adaptive AR modeling of nonstationary time series by means of Kalman filtering. *IEEE Trans. Biomed. Eng.* **45**, 553–562 (1998).
16. Rockstroh, B., Elbert, T., Canavan, A., Lutzenberger, W. & Birbaumer, N. *Slow Cortical Potentials and Behaviour* (Urban & Schwarzenberg, Munich, 1989).
17. Waschulewski, Floruss, H., Miltner, W., Brody, S. & Braun, C. Classical conditioning of pain responses. *Int. J. Neurosci.* **78**, 21–32 (1994).
18. Gray, C. M. & McCormick, D. A. Chattering cells: superficial pyramidal neurons contributing to the generation of synchronous oscillations in the visual cortex. *Science* **274**, 109–113 (1996).
19. Gray, C. M., König, P., Engel, A. K. & Singer, W. Oscillatory responses in cat visual cortex exhibit inter-columnar synchronization which reflects global stimulus properties. *Nature* **338**, 334–337 (1989).
20. Jefferys, J. G., Traub, R. D. & Whittington, M. A. Neuronal networks for induced '40 Hz' rhythms. *Trends Neurosci.* **19**, 202–208 (1996).
21. Traub, R. D., Whittington, M. A., Stanford, I. M. & Jefferys, J. G. A mechanism for generation of long-range synchronous fast oscillations in the cortex. *Nature* **383**, 621–624 (1996).
22. Bromm, B. & Meier, W. The intracutaneous stimulus: a new pain model for algometric studies. *Meth. Find. Exp. Clin. Pharmacol.* **6**, 405–410 (1984).
23. Gratton, G., Coles, M. G. & Donchin, E. A new method for off-line removal of ocular artifact. *Electroencephalogr. Clin. Neurophysiol.* **55**, 468–484 (1983).
24. Perrin, F., Pernier, J., Bertrand, O. & Echallier, J. F. Spherical splines for scalp potential and current density mapping. *Electroencephalogr. Clin. Neurophysiol.* **72**, 184–187 (1989).
25. Biggins, C. A., Fein, G., Raz, J. & Amir, A. Artificially high coherences result from using spherical spline computation of scalp current density. *Electroencephalogr. Clin. Neurophysiol.* **79**, 413–419 (1991).
26. Perrin, F. Comments on article by Biggins et al. *Electroencephalogr. Clin. Neurophysiol.* **83**, 171–174 (1992).
27. Haykin, S. *Adaptive Filter Theory* (Prentice-Hall, Englewood Cliffs, New Jersey, 1986).
28. Chen, H. H. & Guo, L. *Identification and Stochastic Adaptive Control* (Birkhäuser, Boston, Massachusetts, 1991).

**Acknowledgements.** We thank I. Gutberlet for assistance in data analysis. This research was supported by a grant from the Deutsche Forschungsgemeinschaft to W.H.R.M. and a grant from the Rehabilitation Research and Development service, US Department of Veterans Affairs to E.T.

Correspondence and requests for materials should be addressed to W.H.R.M. (email: miltner@biopsy.uni-jena.de).

## Origin of HIV-1 in the chimpanzee *Pan troglodytes troglodytes*

Feng Gao\*, Elizabeth Bailes†, David L. Robertson‡, Yalu Chen\*, Cynthia M. Rodenburg\*, Scott F. Michael\*§, Larry B. Cummins||, Larry O. Arthur¶, Martine Peeters#, George M. Shaw\*☆, Paul M. Sharp† & Beatrice H. Hahn\*

\* Departments of Medicine and Microbiology, University of Alabama at Birmingham, 701 S. 19th Street, LHRB 613, Birmingham, Alabama 35294, USA

† Institute of Genetics, University of Nottingham, Queens Medical Centre, Nottingham NG7 2UH, UK

‡ Laboratory of Structural and Genetic Information, CNRS, Marseilles 13402, France

§ Southwest Foundation for Biomedical Research, San Antonio, Texas 78245, USA

¶ AIDS Vaccine Program, National Cancer Institute-Frederick Cancer Research and Development Center, SAIC Frederick, Frederick, Maryland 21702, USA

# Laboratoire Retrovirus, ORSTOM, BP 5045, Montpellier 34032, France

☆ Howard Hughes Medical Institute, University of Alabama at Birmingham, Birmingham, Alabama 35294, USA

**The human AIDS viruses human immunodeficiency virus type 1 (HIV-1) and type 2 (HIV-2) represent cross-species (zoonotic) infections<sup>1–4</sup>. Although the primate reservoir of HIV-2 has been clearly identified as the sooty mangabey (*Cercocebus atys*)<sup>2,4–7</sup>, the origin of HIV-1 remains uncertain. Viruses related to HIV-1 have been isolated from the common chimpanzee (*Pan troglodytes*)<sup>8,9</sup>, but only three such SIVcpz infections have been documented<sup>1,10,11</sup>, one of which involved a virus so divergent<sup>11</sup> that it might represent a different primate lentiviral lineage. In a search for the HIV-1 reservoir, we have now sequenced the genome of a new SIVcpz**

§ Present address: Department of Tropical Medicine, Tulane University, New Orleans, Louisiana 70112, USA.

strain (SIVcpzUS) and have determined, by mitochondrial DNA analysis, the subspecies identity of all known SIVcpz-infected chimpanzees. We find that two chimpanzee subspecies in Africa, the central *P. t. troglodytes* and the eastern *P. t. schweinfurthii*, harbour SIVcpz and that their respective viruses form two highly divergent (but subspecies-specific) phylogenetic lineages. All HIV-1 strains known to infect man, including HIV-1 groups M, N and O, are closely related to just one of these SIVcpz lineages, that found in *P. t. troglodytes*. Moreover, we find that HIV-1 group N is a mosaic of SIVcpzUS- and HIV-1-related sequences, indicating an ancestral recombination event in a chimpanzee host. These results, together with the observation that the natural range of *P. t. troglodytes* coincides uniquely with areas of HIV-1 group M, N and O endemicity, indicate that *P. t. troglodytes* is the primary reservoir for HIV-1 and has been the source of at least three independent introductions of SIVcpz into the human population.

Five lines of evidence have been used to substantiate zoonotic transmission of primate lentiviruses<sup>3</sup>: first, similarities in viral genome organization; second, phylogenetic relatedness; third, prevalence in the natural host; fourth, geographic coincidence; and fifth, plausible routes of transmission. For HIV-2, a virus (SIVsm) that is genomically indistinguishable and closely related phylogenetically was found in substantial numbers of wild-living sooty mangabeys whose natural habitat coincides with the epicentre of the HIV-2 epidemic<sup>2,4-7</sup>. Close contact between sooty mangabeys and humans is common because these monkeys are hunted for food and kept as pets<sup>6,7</sup>. No fewer than six independent transmissions of SIVsm to humans have been proposed<sup>4,6,7</sup>. In contrast, the origin of HIV-1 is much less certain<sup>3</sup>. HIV-1 is most similar in sequence and genomic organization to viruses found in chimpanzees (SIVcpz)<sup>1,10,11</sup>, but a wide spectrum of diversity between HIV-1 and SIVcpz<sup>11</sup>, an apparent low prevalence of SIVcpz infection in wild-living animals<sup>8,9,12</sup>, and the presence of chimpanzees in geographic regions of Africa<sup>13</sup> where AIDS was not initially recognized have cast doubt on chimpanzees as a natural host and reservoir for HIV-1. Rather, it has been suggested that another, as yet unidentified, primate species could be the natural host for SIVcpz and HIV-1 (refs 1, 11).

We recently identified a fourth chimpanzee with natural SIVcpz infection. This animal (Marilyn) was wild-caught in Africa (country of origin unknown), exported to the United States as an infant, and used as a breeding female in a primate facility until her death at age 26 years<sup>12</sup>. During a serosurvey in 1985, Marilyn was the only chimpanzee of 98 tested who had antibodies strongly reactive with HIV-1 by enzyme-linked immunosorbent assay (ELISA) and western immunoblot<sup>12</sup>. She had never been used in AIDS research and had not received human blood products after 1969. She died in 1985 after giving birth to still-born twins. An autopsy revealed endometritis, retained placental elements and sepsis as the final cause of death. Depletion of lymphoid tissues was not noted. Here we used the polymerase chain reaction (PCR) to amplify HIV- or SIV-related DNA sequences directly from uncultured (frozen) spleen and lymph-node tissue obtained at autopsy in order to characterize the infection responsible for Marilyn's HIV-1 seropositivity. Amplification and sequence analysis of subgenomic *gag* (508 base pairs (bp)) and *pol* (766 bp) fragments revealed the presence of a virus related to, but distinct from, known SIVcpz and HIV-1 strains. Because virus isolation from the autopsy tissues was unsuccessful, we used PCR to amplify and sequence four overlapping subgenomic fragments that together comprised a complete proviral genome, which we termed SIVcpzUS. Analysis of potential coding regions revealed the presence of a *vpu* gene (found only in HIV-1 and SIVcpz viruses)<sup>11,14</sup> in addition to structural and regulatory genes common to all primate lentiviruses. None of the genes in SIVcpzUS contained deletions, insertions or rearrangements, and all reading frames were open except for *gag* (p24) and *rev* (second exon), which contained single in-frame stop

codons. Promoter and enhancer elements of the SIVcpzUS long terminal repeat (LTR) were indistinguishable from those of other members of the HIV-1/SIVcpz group.

Only three other SIVcpz strains have been reported, two from

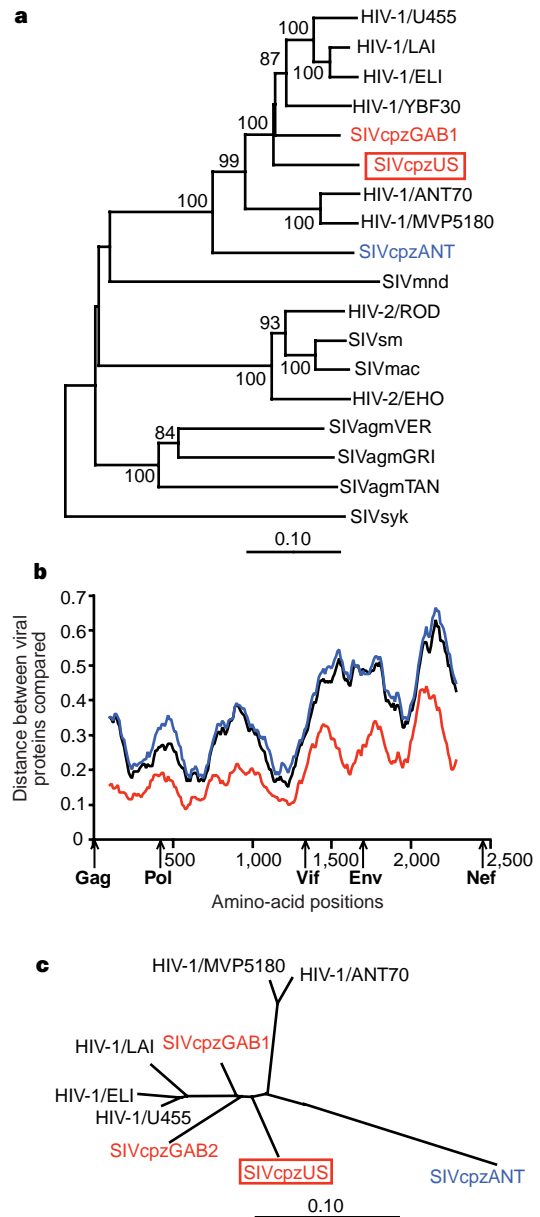


**Figure 1** Phylogenetic analysis of SIVcpzUS. **a**, Phylogenetic relationship of SIVcpzUS to other primate lentiviruses. The tree was derived by neighbour-joining analysis<sup>27</sup> of full-length Pol sequences (trees derived by maximum-likelihood methods<sup>28</sup> yielded very similar topologies). Horizontal branch lengths are drawn to scale with the bar indicating 0.1 amino-acid replacements per site. Numbers at each node indicate the percentage of bootstrap samples (out of 1,000) in which the cluster to the right is supported (only values >80% are shown). Other SIVcpz strains closely or more distantly related to SIVcpzUS are shown in red and blue, respectively. **b**, Diversity plots of concatenated SIVcpz protein sequences depicting the proportion of amino-acid sequence differences between SIVcpzUS and SIVcpzGAB1 (red), SIVcpzUS and SIVcpzANT (blue), and SIVcpzGAB1 and SIVcpzANT (black), calculated for a window of 200 amino acids moved in steps of 10 amino acids along the alignment (available as Supplementary Information). The x-axis shows the amino-acid positions along the alignment. The positions of Gag, Pol, Vif, Env and Nef regions are shown. The y-axis denotes the distance between the viral proteins compared (0.1 = 10% difference). **c**, Unrooted neighbour-joining tree of partial Pol protein sequences (distances are drawn to scale).

animals wild-caught in Gabon (SIVcpzGAB1 and SIVcpzGAB2)<sup>8</sup> and one from a chimpanzee exported to Belgium from Zaire (SIVcpzANT)<sup>9</sup>. SIVcpzGAB1 and SIVcpzANT have been sequenced completely<sup>1,11</sup>, but only 280 bp of *pol* sequence are available for SIVcpzGAB2 (ref. 10). To determine the evolutionary relationships of SIVcpzUS to these and other HIV and SIV sequences, we performed distance plot and phylogenetic tree analyses using sequences from the HIV sequence database (ref. 14 and [http://](http://hiv-web.lanl.gov/HTML/compendium.html)

[hiv-web.lanl.gov/HTML/compendium.html](http://hiv-web.lanl.gov/HTML/compendium.html)). These analyses identified SIVcpzUS unambiguously as a new member of the HIV-1/SIVcpz group of viruses. A phylogenetic tree of full-length *Pol* sequences showed that SIVcpzUS clustered well within this group but was not particularly closely related to any one human or chimpanzee virus (Fig. 1a). Trees based on other coding regions yielded virtually identical topologies (not shown). Comparison of the phylogenetic position of SIVcpzUS with those of the other SIVcpz strains (Fig. 1a)

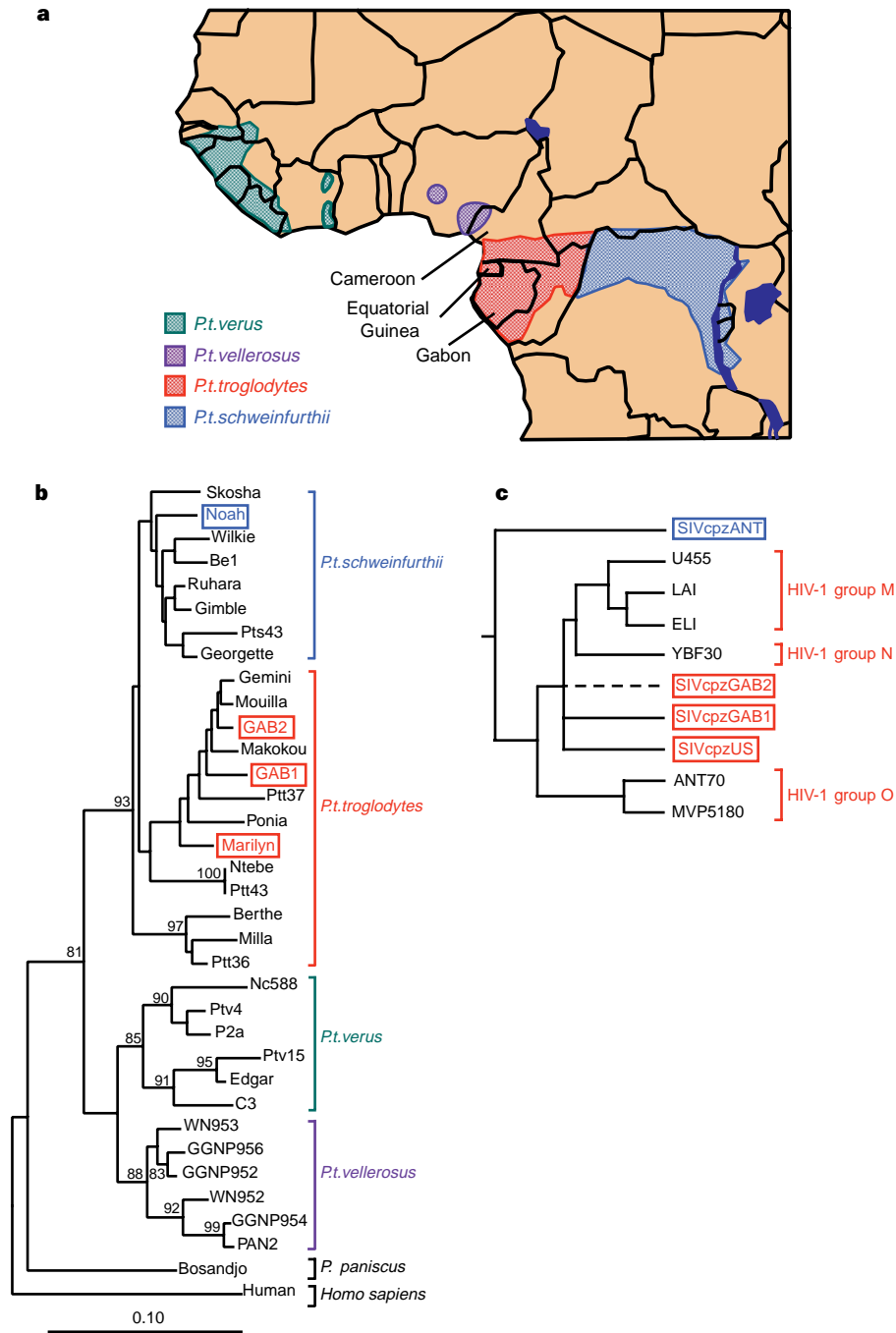


**Figure 2** Origin of HIV-1 in *Pan troglodytes troglodytes*. **a**, Geographic ranges of the four subspecies of the common chimpanzee (*Pan troglodytes*) defined by mtDNA analysis (adapted from refs 19, 20 with permission). **b**, Phylogenetic tree of mtDNA sequences. Positions of sequences from the SIVcpz-infected chimpanzees Marilyn (SIVcpzUS), GAB1 (SIVcpzGAB1), GAB2 (SIVcpzGAB2) and Noah (SIVcpzANT) are boxed. The phylogeny was derived by the neighbour-joining method<sup>27</sup> applied to pairwise sequence distances calculated using the Kimura two-parameter method (transition/transversion ratio set to 10). Horizontal branch lengths are drawn to scale with the bar indicating 0.1 nucleotide

replacements per site. Numbers at each node indicate the percentage of bootstrap samples (out of 1,000) in which the cluster to the right is supported (only values >80% are shown). Brackets on the right indicate previously defined subspecies/species classifications<sup>19,20</sup> (*P. t. troglodytes*, *P. t. schweinfurthii*, *P. t. verus*, and *P. t. vellerosus* are colour coded as in **a**). **c**, Schematic tree of *Pol* sequences, highlighting the position of HIV-1 group M, N and O viruses in relation to *P. t. troglodytes* (red) and *P. t. schweinfurthii* (blue) viruses. The position of SIVcpzGAB2 (indicated by broken line), for which only partial sequence is available<sup>10</sup>, is inferred from the phylogeny shown in Fig. 1c.

showed that SIVcpzUS was considerably more closely related to SIVcpzGAB1 than to SIVcpzANT. Diversity plots of full-length (concatenated) protein sequences showed that SIVcpzUS was nearly twice as different from SIVcpzANT as from SIVcpzGAB1 (Fig. 1b). When partial Pol sequences of SIVcpzGAB2 were included in phylogenetic analyses (Fig. 1c), SIVcpzANT remained the outlier, differing from the other SIVcpz strains by 23–24%, as compared with only 9–13% divergence among SIVcpzUS, SIVcpzGAB1 and SIVcpzGAB2. These findings indicate that naturally occurring SIVcpz strains fall into two related yet highly divergent phylogenetic lineages.

Divergent lineages of SIV have also been found in African green monkeys<sup>15–17</sup>. These primates have a broad distribution throughout sub-Saharan Africa and have been classified based on phenotypic differences into four major species, generally known as vervet (*Chlorocebus pygerythrus*), grivet (*C. aethiops*), sabaues (*C. sabaues*) and tantalus (*C. tantalus*) monkeys (note that the genus designation of the African green monkey as *Cercopithecus* has recently been changed to *Chlorocebus*<sup>18</sup>). The many SIVagm strains infecting these animals cluster in four distinct phylogenetic lineages according to their species of origin, indicating ancient infection followed by co-evolution of virus and host<sup>3,15–17</sup>.

To explore whether a similar host-dependent evolution of SIVcpz could account for the extraordinary diversity between SIVcpzANT and the other three SIVcpz strains, we determined the subspecies identity of the animals from which these viruses were derived. Four chimpanzee subspecies with non-overlapping geographic ranges have been proposed on the basis of genetic differences in mitochondrial (mt) DNA sequences<sup>19,20</sup>. These are the western *P. t. verus*, the Nigerian *P. t. vellerosus*, the central *P. t. troglodytes*, and the eastern *P. t. schweinfurthii* (Fig. 2a). We amplified and sequenced a 498-bp fragment of mitochondrial control region (D-loop) sequences from peripheral-blood mononuclear cell (PBMC) or spleen DNA of the four SIVcpz-infected chimpanzees. Comparison of these newly derived mtDNA sequences to representative sequences from the four chimpanzee subspecies revealed that the three chimpanzees infected with the more closely related SIVcpz-GAB1 (GAB1), SIVcpzGAB2 (GAB2), and SIVcpzUS (Marilyn) strains all belonged to the *P. t. troglodytes* subspecies (Fig. 2b). In contrast, the animal infected with the highly divergent SIVcpzANT strain (Noah) was identified as a member of the *P. t. schweinfurthii* subspecies. Classification of the SIVcpz-infected chimpanzees was unambiguous as their mtDNA sequences fell within well-defined subspecies clusters<sup>19</sup> and was further corroborated by the known geographic origins of three of the animals (GAB1, GAB2 and Noah)<sup>8,9</sup>. We conclude from these results that, as for SIVagm, there has been host-dependent evolution of SIVcpz in chimpanzees.

The discovery of subspecies-specific SIVcpz diversity prompted us to re-examine the phylogenetic positions of all known strains of HIV-1 and SIVcpz, and to look for evidence of cross-species transmission. Globally circulating strains of HIV-1 have been classified into three major phylogenetic groups, termed M, N and O, all of which cause AIDS. The 'main' group M is responsible for the global AIDS epidemic and comprises by far the majority of HIV-1 isolates<sup>21</sup>. These viruses have been further subdivided based on phylogenetic relatedness into ten distinct subtypes or clades, termed A–J (ref. 14). Group O (for 'outlier') is represented by many fewer isolates that originate mainly from Cameroon, Gabon and Equatorial Guinea<sup>22</sup>. Group N (for 'non-M/non-O') was discovered only very recently<sup>23</sup> and is least widespread of all HIV-1 lineages; so far, it has been documented in only two individuals from Cameroon<sup>23</sup>. By comparing the phylogenetic positions of representatives of each of these lineages with those of the four SIVcpz strains, we found that all three HIV-1 groups (M, N and O) clustered closely only with SIVcpz strains infecting chimpanzees of the *P. t. troglodytes* subspecies (Fig. 2c). HIV-1 groups M and N were roughly equidistantly related to SIVcpzGAB1, SIVcpzGAB2 and SIVcpzUS, whereas HIV-1 group O viruses were only slightly more divergent. All SIVcpz strains from

*P. t. troglodytes* and all three groups of HIV-1 formed a single, monophyletic lineage which was supported by highly significant bootstrap values (>90%). This applied for all coding regions and using different phylogenetic methods (Fig. 1a and data not shown). These data indicate strongly that HIV-1 infection of humans occurred as a result of cross-species transmission of SIVcpz from *P. t. troglodytes*.

Two additional lines of evidence supported a *P. t. troglodytes* origin of HIV-1. First, we found that YBF30, the only fully sequenced example of HIV-1 group N (ref. 23), is a recombinant

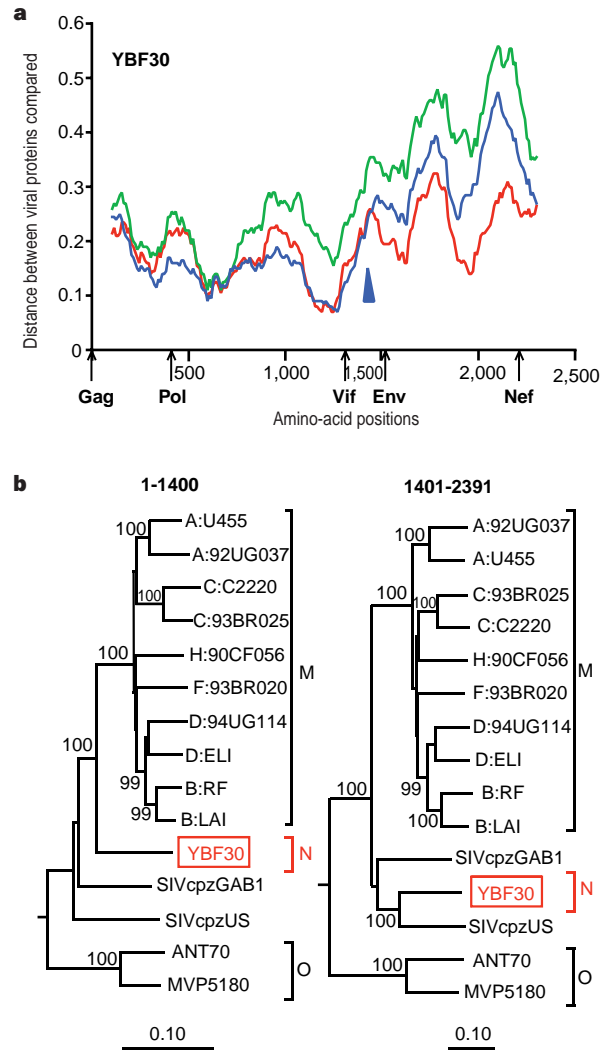


**Figure 3** Recombinant origin of HIV-1/YBF30 (group N). **a**, Diversity plots of concatenated protein sequences, depicting the proportion of amino-acid sequence differences between YBF30 (HIV-1 group N) and SIVcpzUS (red), U455 (HIV-1 group M; blue), and MVP5180 (HIV-1 group O; green), were calculated for a window of 200 amino acids moved in steps of 10 amino acids along an alignment. The x-axis indicates the amino-acid positions along the alignment. The positions of Gag, Pol, Vif, Env and Nef regions are shown. The y-axis denotes the distance between the viral proteins compared (0.1 = 10% difference). A blue marker at position 1,400 delineates 5' and 3' regions of disproportionate sequence similarity between YBF30 and SIVcpzUS. **b**, Phylogenetic position of YBF30 (boxed) in different parts of its genome. Trees were derived by neighbour-joining analysis<sup>27</sup> of concatenated protein sequences flanking the putative recombination breakpoint indicated by the marker in **a** (discordant phylogenies for YBF30 were confirmed by maximum-likelihood methods<sup>28</sup>). Horizontal branch lengths are drawn to scale with the bar indicating 0.1 amino-acid replacements per site; numbers at each node indicate the percentage of bootstrap samples (out of 1,000) in which the cluster to the right is supported (only values >80% are shown). Brackets identify members of HIV-1 groups M, N and O.

of divergent viral lineages within the HIV-1/SIVcpz(*P.t.t.*) group. Distance plots of full-length (concatenated) protein sequences revealed that YBF30 and SIVcpzUS were disproportionately more similar to each other in the 3' half compared to the 5' half of their genome (Fig. 3a). Phylogenetic tree analyses confirmed these discordant relationships, showing that YBF30 fell into significantly different phylogenetic positions in different parts of its genome (Fig. 3b). For example, in *gag*, *pol* and the 5' half of *vif*, YBF30 sequences formed an independent lineage more closely related to HIV-1 group M than to any SIVcpz; however, in the 3' half of *vif*, and in *env* and *nef*, YBF30 clustered most closely with SIVcpzUS. This mosaic genome structure of YBF30 implies previous co-infection and recombination of divergent SIVcpz strains in a *P. t. troglodytes* host. Second, by carefully analysing three full-length SIVcpz genomes for chimpanzee-specific 'signature' sequences, we found a single protein domain, the V3 loop region of the extracellular envelope glycoprotein, to be conserved uniquely among all SIVcpz strains, even the otherwise highly divergent SIVcpzANT. This sequence conservation was most evident in the V3 crown region which was identical among the three chimpanzee viruses (GPGMTFYN) and differed by only a single amino-acid residue in YBF30 (GPAMTFYN). These data indicate that SIVcpz viruses, all of which share this envelope feature, might as a consequence be uniquely adapted for replication in the chimpanzee host and that YBF30, by virtue of its similarity to SIVcpz in V3, may represent a virus lineage most recently transmitted to humans.

As yet, the oldest trace of the AIDS pandemic is from a human blood sample collected in 1959 from west-central Africa<sup>24</sup>, although the precise timing and circumstances of early events in the SIVcpz/HIV-1 zoonosis remain obscure. Previous studies exploring the possible origins of HIV-1 made the important discovery that SIVcpz and HIV-1 are isogenic but provided no convincing evidence for chimpanzees—as opposed to another species—as the natural host and reservoir for the human virus<sup>1</sup>. In fact, the extent of sequence differences that were observed between HIV-1 and SIVcpz, especially in *vpu*, led to the conclusion that SIVcpz-infected chimpanzees were unlikely to be the proximal source of HIV-1 (ref. 1).

We have shown here that all HIV-1 strains are phylogenetically closely related to SIVcpz strains infecting *P. t. troglodytes*, a primate whose natural range coincides precisely with areas of HIV-1 group M, N, and O endemicity<sup>13,21–23</sup>. By demonstrating subspecies-dependent evolution of SIVcpz, we also provide evidence for chimpanzees as a long-standing natural reservoir possibly dating to a period before the divergence of *P. t. troglodytes* and *P. t. schweinfurthii*, which is believed to have occurred several hundred thousand years ago<sup>19</sup>. The detection of recombination among divergent SIVcpz lineages provides further evidence that SIVcpz infection rates in wild-living chimpanzees must have been (and still may be) substantial; a trivial explanation for the observed low frequency of SIVcpz infection in captive chimpanzees<sup>8,9,12</sup> is that such animals were either born in captivity or captured as infants before they matured and had increased risk for SIVcpz infection.

Chimpanzees are commonly hunted for food, especially in west equatorial Africa<sup>13</sup>, and as a consequence represent a ready source for zoonotic transmission of SIVcpz to man. Indeed, the phylogenetic positions of HIV-1 groups M, N and O within the HIV-1/SIVcpz radiation (specifically, the interspersed SIVcpz sequences among each of the three HIV-1 groups shown in Fig. 3b, right panel) indicate that the three HIV-1 groups have each arisen as a consequence of independent zoonotic transmissions of SIVcpz from *P. t. troglodytes* to man. Other explanations for the origin of HIV-1 groups M, N and O, such as viral diversification within human populations or acquisition of virus from still another primate species, are either inconsistent with the phylogenetic data or implausible.

We conclude from our results that *P. t. troglodytes* is the natural host and reservoir for HIV-1. It is still possible, however, that the

other chimpanzee subspecies are also infected with SIVcpz (*P. t. schweinfurthii* is an example) and have transmitted their viruses to humans. Such transmissions have not been detected but could have gone unrecognized because of the explosive spread of HIV-1 group M and the absence of serological tests to distinguish SIVcpz(*P.t.t.*) from other SIVcpz lineages. To understand the full extent of natural SIVcpz infection, and the frequency of zoonotic transmission to humans, it will be necessary to screen free-living adult chimpanzees of all four subspecies as well as human populations from corresponding geographic locales. Such studies will require the cooperation of chimpanzee conservationists, local inhabitants and virologists with a keen sensitivity to protection of this endangered species. Notwithstanding these challenges, studies of the natural history and biology of SIVcpz/HIV-1 in chimpanzees and humans promise to yield new insights into the particular circumstances of cross-species transmission and the basis for HIV-1 pathogenicity in humans. □

## Methods

**PCR amplification and sequence analysis of SIVcpzUS.** A complete genomic sequence of SIVcpzUS was obtained by amplifying four overlapping subgenomic fragments from uncultured spleen DNA using nested PCR (see Supplementary Information for details of primer sequences, PCR strategies and amplification conditions). Amplified fragments were cloned and sequenced using the primer walking approach, cycle sequencing and dye terminator methodologies (GenBank accession number AF103818).

**PCR amplification and sequence analysis of chimpanzee mitochondrial DNA.** A 498-bp segment of the mitochondrial D-loop region (corresponding to positions 15,998–16,497 of the human mitochondrial sequence<sup>25</sup>) was amplified from PBMC (GAB1, GAB2, Noah) or spleen DNA (Marilyn) using single-round PCR (see Supplementary Information) and sequenced without interim cloning (GenBank accession numbers: GAB1/AF102683; GAB2/AF102684; Marilyn/AF102685; Noah/AF102687).

**Sequence comparisons.** SIVcpzUS-predicted protein sequences were aligned with those of other HIV and SIV reference strains<sup>14</sup> using CLUSTAL\_X (ref. 26). Complete proteome alignments were constructed by concatenating Gag, Pol, Vif, Env and Nef alignments (available as Supplementary Information); in the regions of *gag-pol* and *pol-vif* gene overlap, the Gag and Pol sequences, respectively, were excluded. Phylogenetic analyses were done using neighbour-joining and maximum-likelihood methods. The neighbour-joining method<sup>27</sup> was applied to protein-sequence distances calculated by the method of Kimura, with 1,000 bootstrap replicates, as implemented in CLUSTAL\_X. The maximum-likelihood method used the JTT model of amino-acid replacement, was replicated five times with shuffled input order, and was implemented in MOLPHY<sup>28</sup>. MtDNA reference sequences were derived from refs 19, 20.

Received 9 November; accepted 21 December 1998.

- Huet, T., Cheynier, R., Meyerhans, A., Roelants, G. & Wain-Hobson, S. Genetic organization of a chimpanzee lentivirus related to HIV-1. *Nature* **345**, 356–359 (1990).
- Hirsch, V. M., Olmsted, R. A., Murphy-Corb, M., Purcell, R. H. & Johnson, P. R. An African primate lentivirus (SIVsm) closely related to HIV-2. *Nature* **339**, 389–392 (1989).
- Sharp, P. M., Robertson, D. L. & Hahn, B. H. Cross-species transmission and recombination of AIDS viruses. *Phil. Trans. R. Soc. Lond. B* **349**, 41–47 (1995).
- Gao, F. *et al.* Human infection by genetically-diverse SIVsm-related HIV-2 in west Africa. *Nature* **358**, 495–499 (1992).
- Gao, F. *et al.* Genetic diversity of human immunodeficiency virus type 2: evidence for distinct sequence subtypes with differences in virus biology. *J. Virol.* **68**, 7433–7447 (1994).
- Chen, Z. *et al.* Genetic characterization of a new west African simian immunodeficiency virus SIVsm: geographic clustering of household-derived SIV strains with human immunodeficiency virus type 2 subtypes and genetically diverse viruses from a single feral sooty mangabey troop. *J. Virol.* **70**, 3617–3627 (1996).
- Chen, Z. *et al.* Human immunodeficiency virus type 2 (HIV-2) seroprevalence and characterization of a distinct HIV-2 genetic subtype from the natural range of SIV infected sooty mangabeyes. *J. Virol.* **71**, 3953–3960 (1997).
- Peeters, M. *et al.* Isolation and partial characterization of an HIV-related virus occurring naturally in chimpanzees in Gabon. *AIDS* **3**, 625–630 (1989).
- Peeters, M. *et al.* Isolation and characterization of a new chimpanzee lentivirus (simian immunodeficiency virus isolate cpz-ant) from a wild-captured chimpanzee. *AIDS* **6**, 447–451 (1992).
- Janssens, W. *et al.* Phylogenetic analysis of a new chimpanzee lentivirus SIVcpz-gab2 from a wild-captured chimpanzee from Gabon. *AIDS Res. Hum. Retroviruses* **10**, 1191–1192 (1994).
- Vanden Haesevelde, M. M. *et al.* Sequence analysis of a highly divergent HIV-1 related lentivirus isolated from a wild captured chimpanzee. *Virology* **221**, 346–350 (1996).
- Gilden, R. V. *et al.* HTLV-III antibody in a breeding chimpanzee not experimentally exposed to the virus (letter). *Lancet* **i**, 678–679 (1986).

13. Telesi, G. in *Understanding Chimpanzees* (eds Heltne, P. G. & Marquardt, L. A.) 312–353 (Harvard Univ. Press, London, 1989).

14. Kober, B. et al. in *Human Retroviruses and AIDS 1997: A Compilation and Analysis of Nucleic Acid and Amino Acid Sequences* (Theoretical Biology and Biophysics Group, Los Alamos, New Mexico, 1997).

15. Hirsch, V. M. et al. Identification of a new subgroup of SIVagm in tantalus monkeys. *Virology* **197**, 426–430 (1993).

16. Müller, M. C. et al. Simian immunodeficiency viruses from central and western Africa: evidence for a new species-specific lentivirus in tantalus monkeys. *J. Virol.* **67**, 1227–1235 (1993).

17. Jin, M. J. et al. Mosaic genome structure of simian immunodeficiency virus from west African green monkeys. *EMBO J.* **13**, 2935–2947 (1994).

18. Groves, C. P. in *Mammalian Species of World: A Taxonomic and Geographic Reference* (eds Wilson, D. E. & Reader, D. M.) 243–277 (Smithsonian Institution Press, Washington DC, 1993).

19. Morin, P. A. et al. Kin selection, social structure, gene flow, and the evolution of chimpanzees. *Science* **265**, 1193–1201 (1994).

20. Gonder, M. K. et al. A new west African chimpanzee subspecies? *Nature* **388**, 337 (1997).

21. Sharp, P. M., Robertson, D. L., Gao, F. & Hahn, B. H. Origins and diversity of human immunodeficiency viruses. *AIDS* **8**, S27–S42 (1994).

22. Gürtler, L. G. et al. HIV-1 subtype O: epidemiology, pathogenesis, diagnosis, and perspectives of the evolution of HIV. *Arch. Virol. Suppl.* **11**, 195–202 (1996).

23. Simon, F. et al. Identification of a new human immunodeficiency virus type 1 distinct from group M and group O. *Nature Med.* **4**, 1032–1037 (1998).

24. Zhu, T. et al. An African HIV-1 sequence from 1959 and implications for the origin of the epidemic. *Nature* **391**, 594–597 (1998).

25. Anderson, S. et al. Sequence and organization of the human mitochondrial genome. *Nature* **290**, 457–465 (1981).

26. Thompson, J. D., Gibson, T. J., Plewniak, E., Jeanmougin, F. & Higgins, D. G. The CLUSTAL\_X windows interface: flexible strategies for multiple sequence alignment aided by quality analysis tools. *Nucleic Acids Res.* **24**, 4876–4882 (1997).

27. Saitou, N. & Nei, M. The neighbor-joining method: a new method for reconstructing phylogenetic trees. *Mol. Biol. Evol.* **4**, 406–425 (1987).

28. Adachi, J. & Hasegawa, M. MOLPHY (a program package for MOlecular PHYlogenetics), version 2.2 (Institute of Statistical Mathematics, 4-6-7 Minami-Azabu, Minato-ku, Tokyo 106, Japan, 1994).

Supplementary information is available on Nature's World-Wide Web site (<http://www.nature.com>) or as paper copy from the London editorial office of Nature.

**Acknowledgements.** We thank P. Gagneux for mtDNA primer sequences; A. L. Rose, J. Moore and K. Ammann for information concerning chimpanzee hunting practices in west equatorial Africa; T. Goldberg, C. Boesch, R. W. Wrangham, J. Fritz and L. Brent for discussion; B. Jian for technical assistance; and W. J. Abbott and J. B. Wilson for artwork and manuscript preparation. This work was supported by grants from the National Institutes of Health, by shared facilities of the UAB Center for AIDS Research, and by the Birmingham Veterans Administration Medical Center.

Correspondence and requests for materials should be addressed to B.H.H. (e-mail: bhahn@uab.edu).

## Molecular characterization of mitochondrial apoptosis-inducing factor

Santos A. Susin\*, Hans K. Lorenzo†, Naoufal Zamzami\*, Isabel Marzo\*, Bryan E. Snow‡, Greg M. Brothers‡, Joan Mangion‡, Etienne Jacotot\*, Paola Costantini\*, Markus Loeffler\*, Nathanael Larochette\*, David R. Goodlett§, Ruedi Aebersold§, David P. Siderovski‡, Josef M. Penninger‡ & Guido Kroemer\*

\* Centre National de la Recherche Scientifique, UPR 420, 19 rue Guy Môquet, F-94801 Villejuif, France

† Unité de Biochimie Structurale, Institut Pasteur, 25 rue du Dr Roux, F-75724 Paris Cedex 15, France

‡ The Amgen Institute and Ontario Cancer Institute, Department of Medical Biophysics and Immunology, University of Toronto, 620 University Avenue, Suite 706, Toronto, Ontario M5G 2C1, Canada

§ Department of Molecular Biotechnology, University of Washington, Seattle, Washington 98195, USA

Mitochondria play a key part in the regulation of apoptosis (cell death)<sup>1,2</sup>. Their intermembrane space contains several proteins that are liberated through the outer membrane in order to participate in the degradation phase of apoptosis<sup>3–9</sup>. Here we report the identification and cloning of an apoptosis-inducing factor, AIF<sup>5</sup>, which is sufficient to induce apoptosis of isolated nuclei. AIF is a flavoprotein of relative molecular mass 57,000 which shares homology with the bacterial oxidoreductases; it is normally confined to mitochondria but translocates to the nucleus when apoptosis is induced. Recombinant AIF causes chromatin condensation in isolated nuclei and large-scale frag-

mentation of DNA. It induces purified mitochondria to release the apoptogenic proteins cytochrome *c* and caspase-9. Microinjection of AIF into the cytoplasm of intact cells induces condensation of chromatin, dissipation of the mitochondrial transmembrane potential, and exposure of phosphatidylserine in the plasma membrane. None of these effects is prevented by the wide-ranging caspase inhibitor known as Z-VAD.fmk. Overexpression of Bcl-2, which controls the opening of mitochondrial permeability transition pores, prevents the release of AIF from the mitochondrion but does not affect its apoptogenic activity. These results indicate that AIF is a mitochondrial effector of apoptotic cell death.

Opening of the mitochondrial permeability transition pore, which is under the control of members of the Bcl-2 family, is one of the decisive events of the apoptotic process<sup>1,2</sup>, causing an increase in the permeability of the outer mitochondrial membrane<sup>7</sup> and the release of soluble proteins from the intermembrane space. The mitochondrial intermembrane fraction contains several potentially apoptogenic factors, including cytochrome *c* (refs 4, 6), pro-caspases 2, 3 and 9 (refs 8, 9), and AIF, which forces isolated nuclei to adopt an apoptotic morphology<sup>3,5</sup>. We purified an AIF activity that is maintained in the presence of the caspase inhibitor

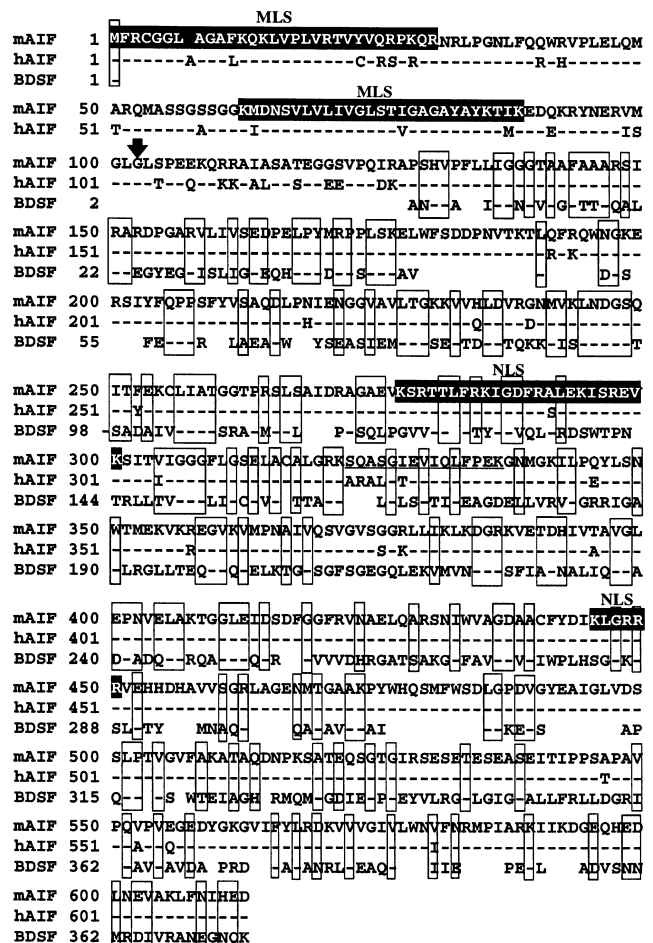


**Figure 1** Alignment of mouse and human AIF amino-acid sequences with benzene 1,2-dioxygenase system ferredoxin NADH reductase from *Pseudomonas putida* (BDSF; 30% amino-acid identity with mouse AIF). Dashes indicate amino-acid identity; lined boxes indicate amino-acid similarity; black boxes highlight mitochondrial localization sequences (MLS; ref. 11) and putative nuclear-localization sequences (NLS; ref. 13). Arrow, first residue (amino acid 102) of mature AIF purified from mouse liver, as determined by N-terminal sequencing. The underlined sequence in mouse AIF matches the mass spectroscopy data obtained with trypsin-digested purified AIF. GenBank accession numbers for mouse and human AIF are AF100927 and AF100928, respectively.